Supplement of Atmos. Chem. Phys., 23, 9401–9411, 2023
https://doi.org/10.5194/acp-23-9401-2023-supplement

Atmospheric Chemistry and Physics
Open Access

Supplement of

A rise in HFC-23 emissions from eastern Asia since 2015

Hyeri Park et al.

Correspondence to: Sunyoung Park (sparky@knu.ac.kr)

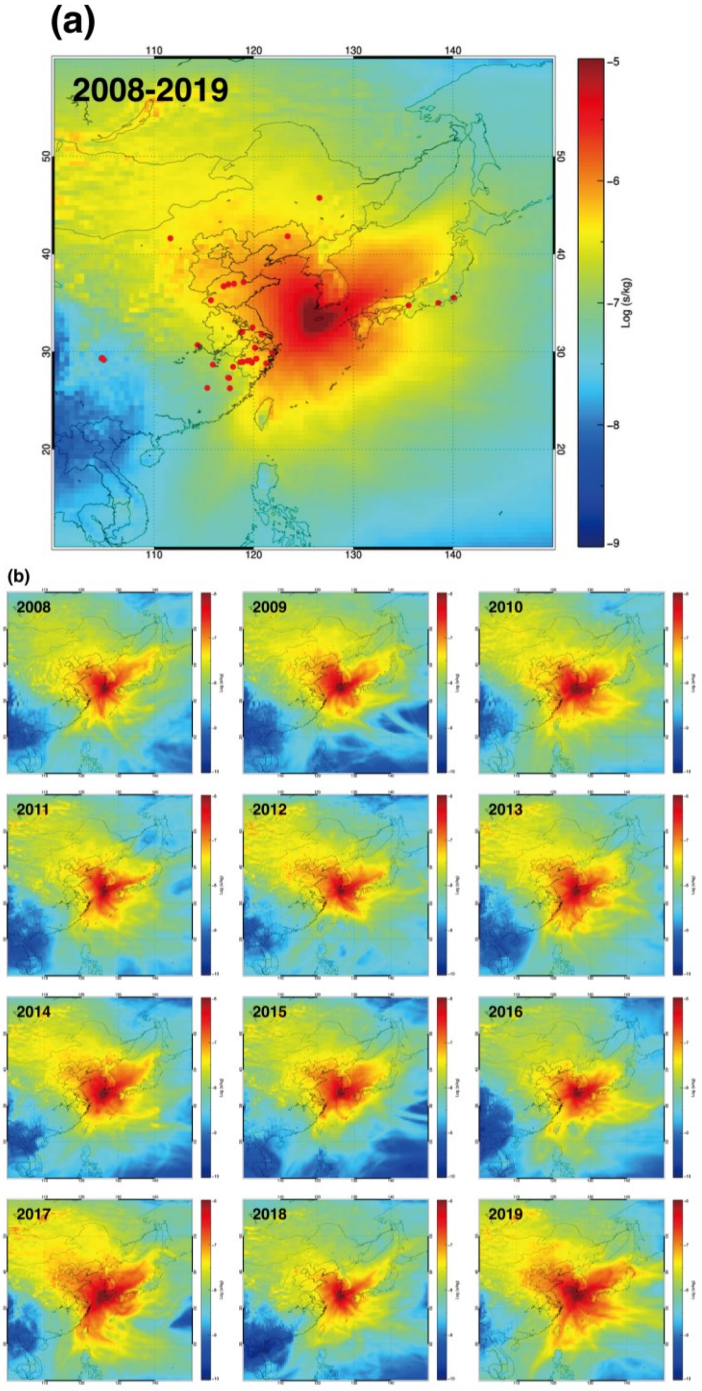

Figure S1: The sensitivity of the measurements to emissions of HFC-23 (a) for 2008-2019 and (b) for each year between 2008–2019. The figure (b) shows that the mean sensitivity of the observations to emissions from the eastern Asia region did not change substantially throughout this period. The red circles indicate locations of known HCFC-22 production plants.

HCFC-22 production in China

Note that under the Montreal Protocol, the use of HCFC-22 as a feedstock has been exempted from the phase-out schedule in some countries, including China. According to the TEAP 2021 report, the proportion of China's HCFC-22 production for feedstock use has been increasing relative to HCFC-22 production for dispersive use (Figure S2). Therefore, the lack of a clear decline in HCFC-22 production even after 2013 (Figure S3) could be due to an increase in production for feedstock use in China.

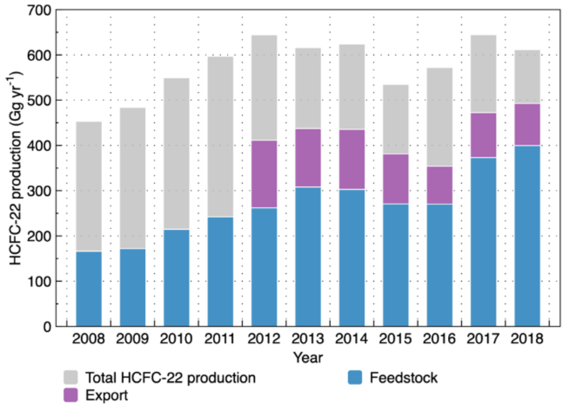

Figure S2: Total HCFC-22 productions of China (stacked bars). Blue segments denote production for feedstock uses and purple for export.

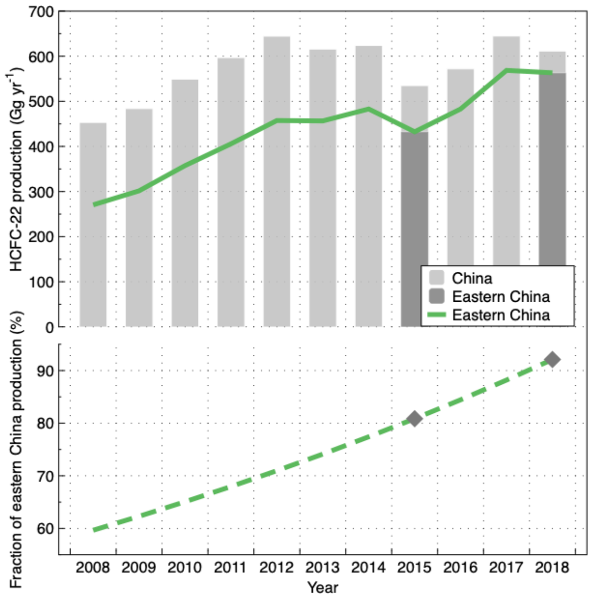

Figure S3: (a) Total HCFC-22 productions of China (light gray bars) and HCFC-22 productions of eastern China in 2015 and 2018 (dark gray bars) (TEAP, 2021). (b) Inferred annual fractions of eastern China HCFC-22 productions to Chinese total productions (dark gray rhombi), extrapolated eastern China HCFC-22 production fractions for other years (green dashed line).

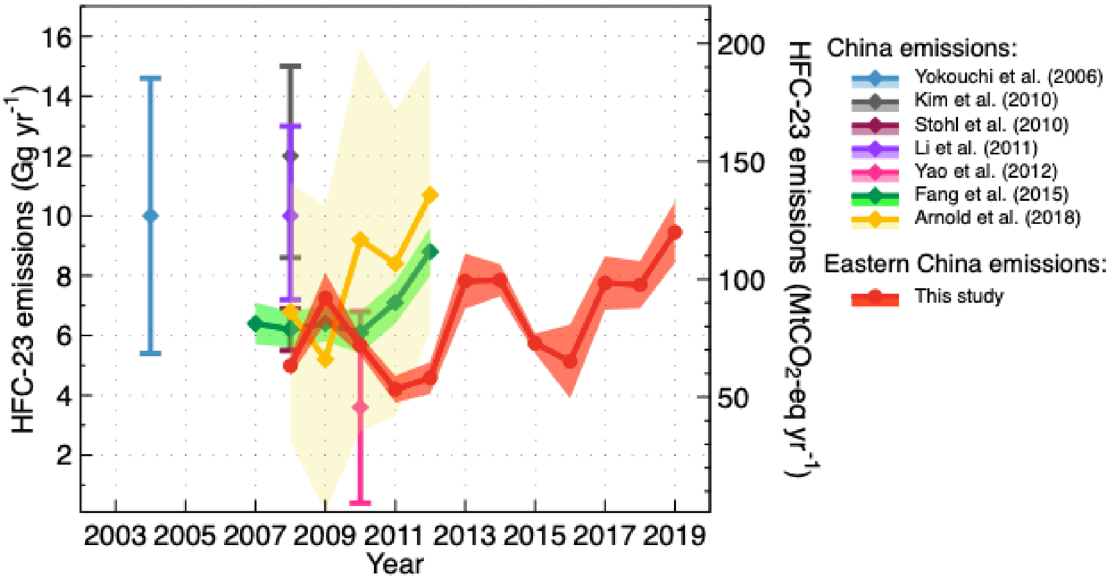

Figure S4: HFC-23 emissions estimates in eastern China (red line), in comparison with previous top-down estimates of Chinese HFC-23 emissions.

Table S1: Information on HCFC-22 production factories in China

	Company Name	Province	Information	Location		CDM Participation Period	HCFC-22 production (ktonnes)
				Lat.	Long.		
1	Jiangsu Meilan Chemical Co., Ltd	Jiangsu	https://cdm.unfccc.int/Projects/DB/JQA1144312006.34/view	32.50	119.89	Dec 2006- Nov 2013	63.9
2	Changshu Haike_3F Changsu	Jiangsu	https://cdm.unfccc.int/Projects/DB/JQA1177467814.44/view	31.78	120.82	May 2008 - Apr 2015	40.9
3	Changshu 3 Zhonghao New Chemical Materials Co. Ltd.	Jiangsu	Company websites	31.81	120.79	–	–
4	Changshu Arkema 3F Fluorine Chemical Co. Ltd.	Jiangsu	TEAP, 2017	31.75	120.80	–	30.7
5	Nanjing Jiling Refrigeration Technology Co., Ltd	Jiangsu	Company websites	32.04	118.77	–	–
6	Jiangsu Huafu Poly Environmental Protection Technology Co., Ltd	Jiangsu	Company websites	32.02	118.86	–	–
7	Shandong Dongyue Chiemical Co., Ltd	Shandong	https://cdm.unfccc.int/Projects/DB/DNV-CUK1136817489.89/view	36.97	118.03	Jan 2007 - Dec 2013	173.3
8	China Fluoro Technology Co., Ltd	Shandong	cdm.unfccc.int/Projects/DB/DNV-CUK1182313000.09/view	36.71	117.00	Sep 2007 - Sep 2014	–
9	Shandong ZhongFu	Shandong	TEAP, 2017	36.90	117.46	–	NaN
10	Jinan 3F Fluoro Chemical Co. Ltd.	Shandong	Company websites	36.69	116.99	–	–
11	Shandong Haihua Group Co. Ltd.	Shandong	Company websites	37.12	118.99	–	–
12	Shandong Danbu Chemical Co., Ltd	Shandong	Company websites	35.27	115.71	–	–
13	Dongyang Chemical Co., Ltd	Zhejiang	Company websites	29.27	120.25	–	–
14	No.1 Zhejian JuHua Co., Ltd	Zhejiang	https://cdm.unfccc.int/Projects/DB/DNV-CUK1135255248.44/view	28.90	118.90	Aug 2006- July 2013	–
15	No. 2 Zhejian JuHua Co., Ltd	Zhejiang	https://cdm.unfccc.int/Projects/DB/SGS-UKL1169224204.45/view	28.90	118.90	Apr 2007 - Apr 2014	–
16	Zhengjiang Quhua Co., Ltd	Zhejiang	TEAP, 2017	28.91	118.87	–	49.2
17	Zhejiang Lanxi Juhua Fluorine Chemicals Co., Ltd.	Zhejiang	TEAP, 2017	29.22	119.44	–	20.6
18	Yingpeng Chemical Co., Ltd	Zhejiang	cdm.unfccc.int/Projects/DB/DNV-CUK1215776483.62/view	28.90	120.01	Apr 2009 - Apr 2016	–
19	Limin Chemical Co., Ltd	Zhejiang	https://cdm.unfccc.int/Projects/DB/JQA1154594999.24/view	34.37	118.32	Jan 2007 - Dec 2013	17.5
20	Zhejiang Dongyang Chemical Co., Ltd	Zhejiang	https://cdm.unfccc.int/Projects/DB/JQA1154593239.79/view	29.27	120.25	Nov 2006 - Oct 2013	–
21	Zhejiang Sanmei Chemical Incorporated Company	Zhejiang	TEAP, 2017	28.89	119.83	–	14.4
22	Zhejian Pengyou	Zhejiang	TEAP, 2017	29.09	119.61	–	10
23	Jinhua Yonghe Fluorochemical	Zhejiang	TEAP, 2017	29.07	119.38	–	12
24	Zhejiang Jusheng Fluorochemical Co.=Zhejian Quhua	Zhejiang	Inside Climate News	28.97	118.87	–	–
25	Zhejiang Yonghe New type Refrigerant Co. Ltd.	Zhejiang	Company websites	28.95	118.92	–	–
26	Ningbo Koman's Refrigeration Industry Co. Ltd.	Zhejiang	Company websites	29.88	121.88	–	–
27	Quzhou saitel Chemical Co., Ltd	Zhejiang	Company websites	28.93	118.66	–	–
28	Hangzhou Wula Chemical Co., Ltd	Zhejiang	Company websites	30.40	120.14	–	–
29	Dongyang Chemical Co., Ltd	Zhejiang	Company websites	29.27	120.25	–	–
30	Fujian Shaowu Youghe Jintang New Materials Co.	Fujian	Inside Climate News	27.30	117.55	–	–
31	Fujian Sannong New Materials Co., Ltd	Fujian	Inside Climate News	26.26	117.61	–	–
32	Fujian Haidefu New Materials Co., Ltd	Fujian	Inside Climate News	27.34	117.44	–	–
33	Changjiang Chemical Plant	Hubei	Company websites	30.68	114.37	–	–
34	Harbin Sanyi Refrigeration Equipment Co., Ltd	Heilongjiang	Company websites	45.75	126.60	–	–
35	Inner Mongolia Yonghe Fluorochemical Co., Ltd	Inner Mongolia	Inside Climate News	41.61	111.64	–	–
36	Jingxi YingGuang	Jiangxi	TEAP, 2017	28.45	117.93	–	0
37	Jiangxi Sanmei Chemical	Jiangxi	TEAP, 2017	26.29	115.35	–	14
38	Shenyang Guyun Refrigeration Equipment Co., Ltd	Liaoning	Company websites	41.82	123.41	–	–
39	Zhonghao Chenguang Research Institute of Chemical Industry	Sichuan	https://cdm.unfccc.int/Projects/DB/JQA1163409153.5/view	29.17	104.97	May 2007 - Apr 2014	17.2
40	Sichuan Zigong Honghe Chemical Co., Ltd.	Sichuan	TEAP, 2017	29.35	104.80	–	NaN
41	Zigong City refrigerant factory	Sichuan	Company websites	29.31	104.73	–	–
42	Zigong City reactor Chemical plant	Sichuan	Company websites	29.35	104.77	–	–

Observations of atmospheric HCFC-22 and estimation of top-down emissions in eastern China

High-frequency observation data of HCFC-22 at Gosan for 2008-2018 (Figure S6) show persistent pollution events, clearly implying that HCFC-22 emissions have been emanating from the surrounding regions, while the regional baseline concentrations of HCFC-22 show a similar increasing trend as the global NH baseline (green dots in Figure S6 for the Mace Head station). It should be noted that HCFC-22 baseline concentrations at Gosan drop periodically in summer due to strong intrusion of SH tropical air masses with low HCFC-22 concentrations during the East Asia summer monsoon (Li et al., 2018).

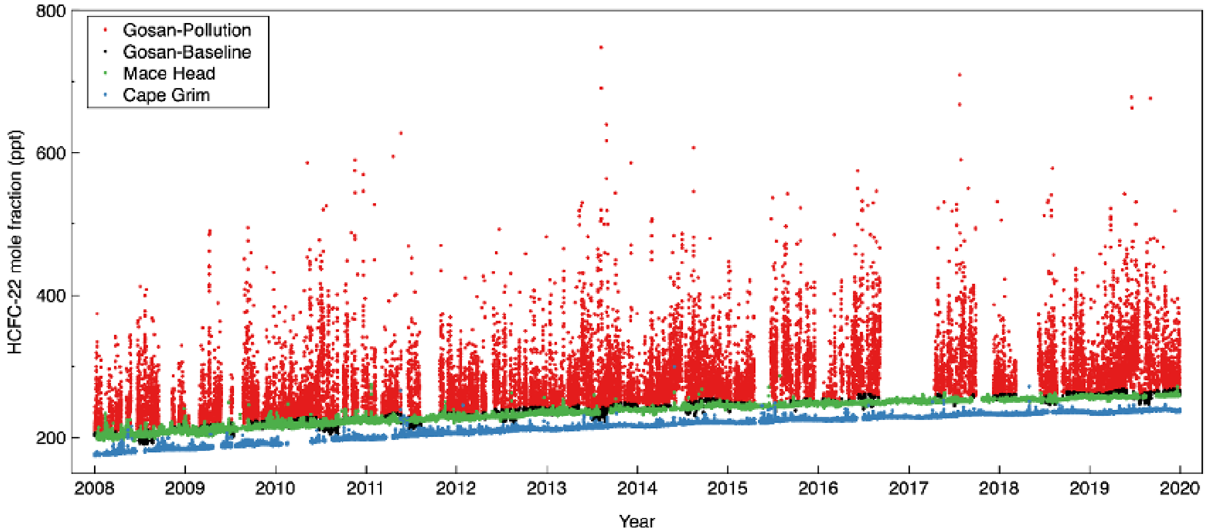

Figure. S5: Atmospheric HCFC-22 concentrations observed from 2008 to 2019 at Gosan. The green and blue dots show HCFC-22 concentrations observed at Mace Head and Cape Grim, respectively, for comparison.

To confirm the link of HFC-23 emissions in eastern China to HCFC-22 production, we estimated HCFC-22 emissions from eastern China using the same inverse framework as for HFC-23 (Figure S7(a)). The continuing rise in the emissions seems to indicate that the contribution of dispersive use is still significant, although its production for dispersive use is currently being phased out in developing countries by the Montreal Protocol. HCFC-22 emissions from the whole of China were inferred from the faction of the population in eastern China. Results are consistent not only with previous studies but also with the inventory-based HCFC-22 emissions as shown in Figure S7(b), suggesting that population density still serves as good proxy for HCFC-22 emissions, and that the bottom-up emissions for the whole of China are relatively well-defined.

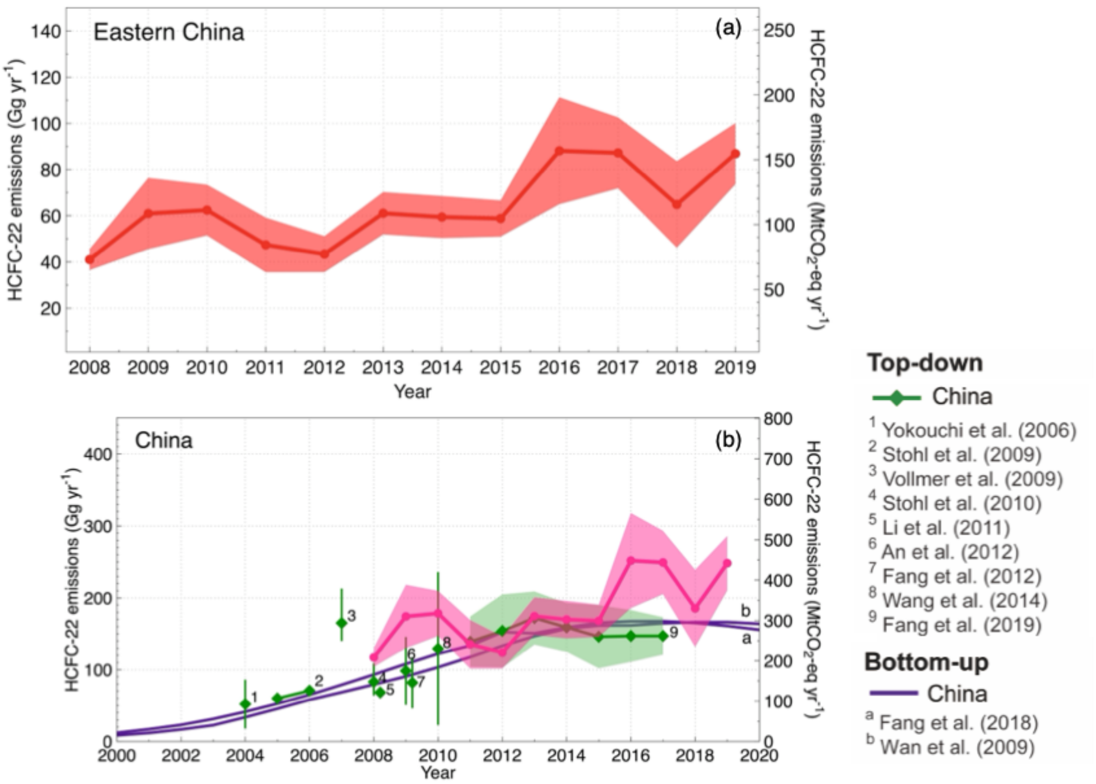

Figure S6: (a) Eastern Chinese emissions of HCFC-22 (red circles) derived from the atmospheric observations at Gosan, (b) Our HCFC-22 emission estimates by the whole of China (pink circles), determined by scaling up the eastern Chinese emissions by the fraction of the population (35 %) that reside in eastern China (Rigby et al., 2019). Top-down Chinese emissions suggested in previous studies and bottom-up estimates are denoted by green rhombi and purple lines, respectively.

Three different spatial distributions of *a priori* emissions

Our inverse modelling results represent the mean and 2-σ uncertainty of 27 different model runs, where each set of three different *a priori* distributions (Figure S8) have 9 combinations of different *a priori* emission magnitudes. The first priori distribution is the "Population" *a priori*, determined based on the 2010 World population distribution (Warszawski et al., 2017). Population distribution has often been used as a reasonable first approximation when more specific information is not available (Stohl et al., 2010; Fang et al., 2019). The second priori distribution is the "Asiaflat" *a priori*, where the emissions within each country (whole of China, North Korea, South Korea, and whole of Japan) were evenly spread (Rigby et al., 2019; Park et al., 2021). This flattening may cause large *a priori* emissions to be allocated to western China and eastern Japan, where transport sensitivity was relatively low, while at the same time significantly lowering *a priori* emissions in eastern China and western Japan compared to other *a priori* distributions (Kim et al., 2021). The third priori distribution is the "EastAsiaflat" *a priori*, where the population distribution-based emissions are regionally flattened. Flatting regions are determined as the high sensitivity in the model domain (most of the high sensitivity area has less than or equal to 1° by 1°), i.e., eastern China, South Korea, North Korea, and western Japan. The region denoted "eastern China" contains nine provinces (Anhui, Beijing, Hebei, Jiangsu, Liaoning, Shandong, Shanghai, Tianjin, and Zhejiang) and "western Japan" contains four regions (Chūgoku, Kansai, Kyūshū & Okinawa and Shikoku) (Rigby et al., 2019; Park et al., 2021; Kim et al., 2021). "EastAsiaflat" *a priori* can be unbiased in terms of emission locations, such that the distribution of emissions in the posterior could point to likely emission hot spots, but such inference is reasonable only in regions where the influence of the observations is relatively strong. The *a priori* emissions were kept constants for all years, based on the 2008 emissions. For each *a priori* distribution, we tested 9 different combinations of *a priori* emission magnitudes and uncertainties, which are summarized in Table S2.

Note that our annual HFC-23 results represent the mean of 18 results from two different model runs *a priori* excluding "Asiaflat" *a priori*, because many HCFC-22 factories are located in eastern China, and thus HFC-23 emissions estimates for eastern China using "Asiaflat" *a priori* could be underestimated.

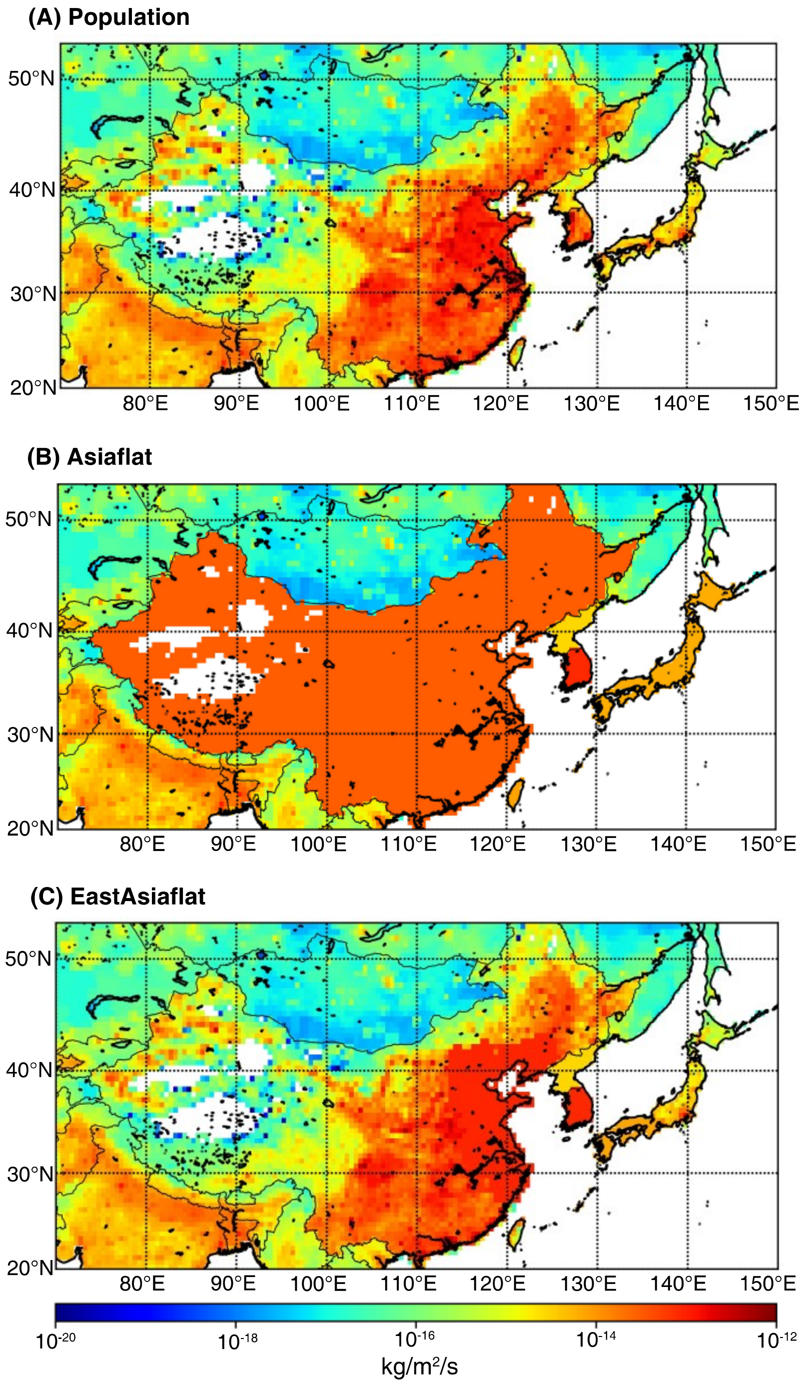

Figure S7: Three different spatial distributions of *a priori* used in this study. (a) *a priori* emissions map based on populations distribution. (b) flat emissions for each country. (c) flat emissions only in the regions with high sensitivity (eastern China, North Korea, South Korea and western Japan).

Table S2: List of 9 *a priori* configurations, with corresponding errors, applied to each *a priori* distribution. For each *a priori* configuration, the initial *a priori* estimate is multiplied by the listed scaling factor.

***A priori* Emissions**								
A priori Dist.	priori	Error (%)	priori Dist.	priori	Error (%)	priori Dist.	priori	Error (%)
Population	× 0.5	100	Asiaflat	× 0.5	100	EastAsiaflat	× 0.5	100
	× 1	50		× 1	50		× 1	50
	× 2	25		× 2	25		× 2	25
	× 0.5	200		× 0.5	200		× 0.5	200
	× 1	100		× 1	100		× 1	100
	× 2	50		× 2	50		× 2	50
	× 0.5	300		× 0.5	300		× 0.5	300
	× 1	150		× 1	150		× 1	150
	× 2	75		× 2	75		× 2	75

Model validation based on CFC-11 emissions estimate from eastern China

To validate the optimization of our inversion framework, we analyzed CFC-11 emissions from eastern China using Gosan CFC-11 concentration data for 2008–2019. Top-down emissions of CFC-11 in East Asia were well-defined in a recent study (Park et al., 2021) which used multiple inversion methods.

Our results (Figure S9) showed good convergence among the runs for the same *a priori* distribution set, but relatively large (not statistically significant) difference between different *a priori* distributions, suggesting that *a priori* distributions have an impact on the a posteriori, and thus uncertainties associated with different *a priori* settings need to be considered to derive the full posteriori uncertainties.

Figure S10 shows that our CFC-11 emission estimates for eastern China are consistent within uncertainties with previously reported results from four different inverse methods that used Gosan observation data (only) (Park et al., 2021). Since the previous study with four different inverse models had used “Asiaflat” *a priori*, our estimation was also made with the same priori for direct comparison.

We took the mean of the a posteriori annual inversion results from 27 independent inversions with different *a priori* settings (see Table S2) as our final estimates of CFC-11 emissions from eastern China for 2008–2019 (Figure S11 and Table S3) and their uncertainties were defined as 2-σ of the resulting a posteriori emissions (95 % uncertainty), because the uncertainty of each inversion run can be considered fully correlated with each other. Our final emissions estimates of CFC-11 for eastern China are also consistent with previously reported results from four different inverse methods within uncertainties (Figure S11).

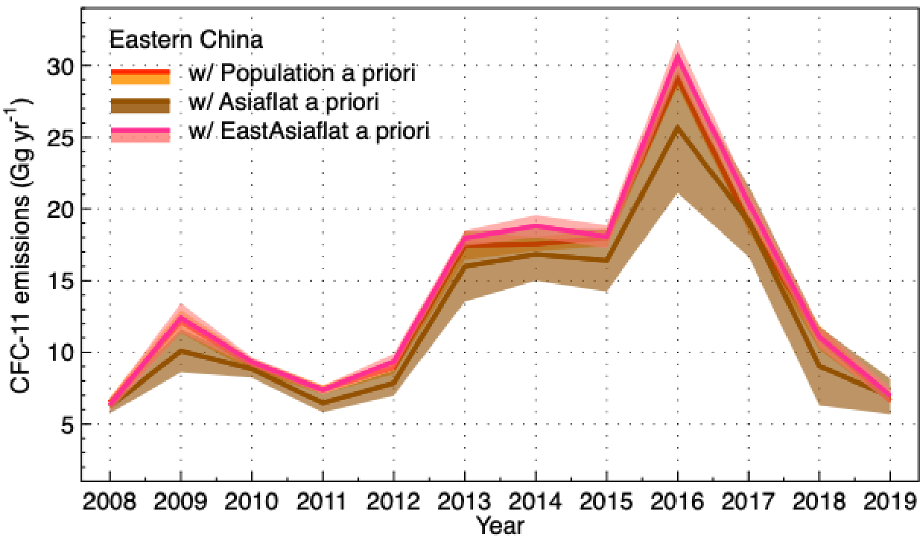

Figure S8: CFC-11 emissions from eastern China derived using three different *a priori* distributions: “Population”, “Asiaflat”, “EastAsiaflat” *a prioris*. Each line represents the annual mean of 9 different model set-ups for each *a priori* distribution. Shading denotes 2-σ uncertainties.

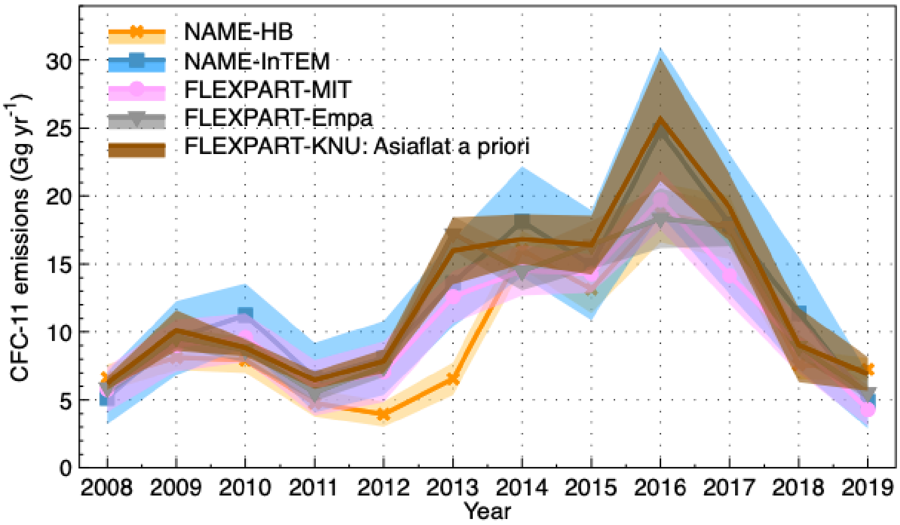

Figure S9: CFC-11 emissions from eastern China derived using the "Asiaflat" *a priori* distribution. Top-down emissions using FLEXPART-KNU (brown line) are compared to previously reported emissions from four different inverse methods using the same Gosan data for 2008–2019: NAME-HB (yellow crosses), NAME-InTEM (blue squares), FLEXPART-MIT (pink circles) and FLEXPART-Empa (gray triangles).

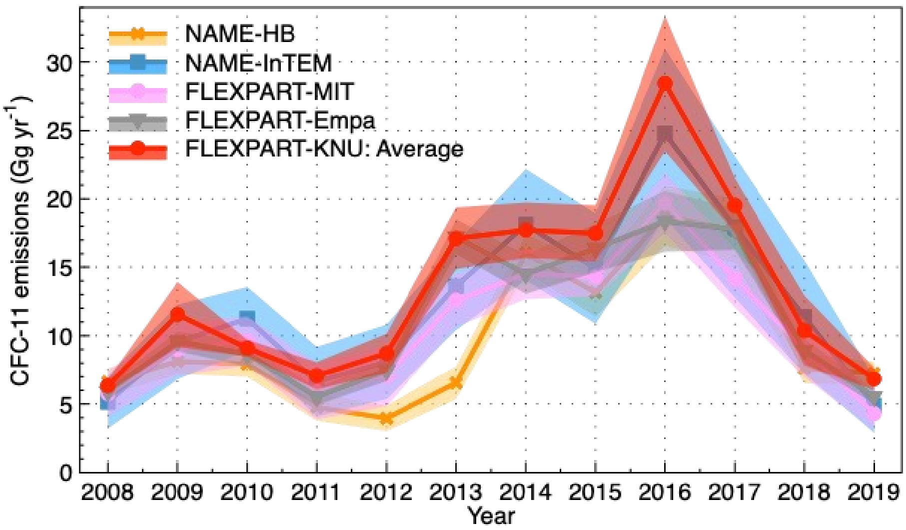

Figure S10: CFC-11 emissions estimate for eastern China derived in this study (FLEXPART-KNU, red circles) compared to previously derived emissions. Our annual results represent the mean of 27 different model runs, where each set of three different *a priori* distributions have 9 combinations of different emission magnitudes and 2-σ uncertainties (shading).

Table S3: Top-down emissions (Gg yr^{-1}) of CFC-11 and HCFC-22 for eastern China

Year	CFC-11			HCFC-22		
	Eastern China			Eastern China		
	mean	max	min	mean	max	min
2008	6.34	6.81	5.86	40.99	45.53	36.44
2009	11.55	13.92	9.18	60.96	76.40	45.51
2010	9.09	9.70	8.48	62.45	73.46	51.44
2011	7.08	8.07	6.09	47.36	59.20	35.52
2012	8.72	10.15	7.29	43.37	51.17	35.56
2013	17.12	19.39	14.85	61.07	70.27	51.87
2014	17.73	19.73	15.72	59.43	68.57	50.30
2015	17.48	19.54	15.43	58.80	66.67	50.93
2016	28.44	33.39	23.48	88.13	111.27	64.98
2017	19.53	21.49	17.56	87.23	102.62	71.84
2018	10.38	12.92	7.84	64.89	83.67	46.12
2019	6.84	7.66	6.01	86.89	100.13	73.64

SI. References

An, X., Henne, S., Yao, B., Vollmer, M. K., Zhou, L., and Li, Y.: Estimating emissions of HCFC-22 and CFC-11 in China by atmospheric observations and inverse modeling, Science China Chemistry, 55, 2233-2241, 2012.

Arnold, T., Manning, A. J., Kim, J., Li, S., Webster, H., Thomson, D., Mühle, J., Weiss, R. F., Park, S., and O'doherty, S.: Inverse modelling of CF4 and NF3 emissions in East Asia, Atmospheric Chemistry and Physics, 18, 13305-13320, 2018.

Fang, X., Wu, J., Su, S., Han, J., Wu, Y., Shi, Y., Wan, D., Sun, X., Zhang, J., and Hu, J.: Estimates of major anthropogenic halocarbon emissions from China based on interspecies correlations, Atmospheric environment, 62, 26-33, 2012.

Fang, X., Stohl, A., Yokouchi, Y., Kim, J., Li, S., Saito, T., Park, S., and Hu, J.: Multiannual top-down estimate of HFC-23 emissions in East Asia, Environmental Science & Technology, 49, 4345-4353, 2015.

Fang, X., Ravishankara, A., Velders, G. J., Molina, M. J., Su, S., Zhang, J., Hu, J., and Prinn, R. G.: Changes in emissions of ozone-depleting substances from China due to implementation of the Montreal Protocol, Environmental science & technology, 52, 11359-11366, 2018.

Fang, X., Yao, B., Vollmer, M., Reimann, S., Liu, L., Chen, L., Prinn, R., and Hu, J.: Changes in HCFC emissions in China during 2011–2017, Geophysical Research Letters, 46, 10034-10042, 2019.

Inside Climate News: China Moves to Freeze Production of Climate Super-Pollutants But Lacks a System to Monitor Emissions, 2022. https://insideclimatenews.org/news/21012022/china-super-pollutant-emissions/

Kim, J., Li, S., Kim, K. R., Stohl, A., Mühle, J., Kim, S. K., Park, M. K., Kang, D. J., Lee, G., and Harth, C. M.: Regional atmospheric emissions determined from measurements at Jeju Island, Korea: Halogenated compounds from China, Geophysical Research Letters, 37, 2010.

Kim, J., Thompson, R., Park, H., Bogle, S., Mühle, J., Park, M. K., Kim, Y., Harth, C. M., Salameh, P. K., and Schmidt, R.: Emissions of tetrafluoromethane (CF4) and hexafluoroethane (C2F6) from East Asia: 2008 to 2019, Journal of Geophysical Research: Atmospheres, 126, e2021JD034888, 2021.

Li, S., Kim, J., Kim, K.-R., Mühle, J., Kim, S.-K., Park, M.-K., Stohl, A., Kang, D.-J., Arnold, T., and Harth, C. M.: Emissions of halogenated compounds in East Asia determined from measurements at Jeju Island, Korea, Environmental science & technology, 45, 5668-5675, 2011.

Li, S., Park, S., Lee, J.-Y., Ha, K.-J., Park, M.-K., Jo, C., Oh, H., Mühle, J., Kim, K.-R., and Montzka, S.: Chemical evidence of inter-hemispheric air mass intrusion into the Northern Hemisphere mid-latitudes, Scientific reports, 8, 1-7, 2018.

Park, S., Western, L. M., Saito, T., Redington, A. L., Henne, S., Fang, X., Prinn, R. G., Manning, A. J., Montzka, S. A., and Fraser, P. J.: A decline in emissions of CFC-11 and related chemicals from eastern China, Nature, 590, 433-437, 2021.

Rigby, M., Park, S., Saito, T., Western, L., Redington, A., Fang, X., Henne, S., Manning, A., Prinn, R., and Dutton, G.: Increase in CFC-11 emissions from eastern China based on atmospheric observations, Nature, 569, 546-550, 2019.

Simmonds, P. G., Rigby, M., McCulloch, A., Vollmer, M. K., Henne, S., Mühle, J., O'Doherty, S., Manning, A. J., Krummel, P. B., and Fraser, P. J.: Recent increases in the atmospheric growth rate and emissions of HFC-23 (CHF_3) and the link to HCFC-22 ($CHClF_2$) production, 2018.

Stanley, K. M., Say, D., Mühle, J., Harth, C. M., Krummel, P. B., Young, D., O'Doherty, S. J., Salameh, P. K., Simmonds, P. G., and Weiss, R. F.: Increase in global emissions of HFC-23 despite near-total expected reductions, Nature communications, 11, 1-6, 2020.

Stohl, A., Seibert, P., Arduini, J., Eckhardt, S., Fraser, P., Greally, B., Lunder, C., Maione, M., Mühle, J., and O'doherty, S.: An analytical inversion method for determining regional and global emissions of greenhouse gases: Sensitivity studies and application to halocarbons, Atmospheric Chemistry and Physics, 9, 1597-1620, 2009.

Stohl, A., Kim, J., Li, S., O'Doherty, S., Mühle, J., Salameh, P. K., Saito, T., Vollmer, M. K., Wan, D., and Weiss, R. F.: Hydrochlorofluorocarbon and hydrofluorocarbon emissions in East Asia determined by inverse modeling, Atmospheric Chemistry and Physics, 10, 3545-3560, 2010.

TEAP: Technology and Economic Assessment Panel of the Montreal Protocol: Assessment Report, United Nations Environment Programme, Nairobi, Kenya, 2017.

TEAP: Technology and Economic Assessment Panel of the Montreal Protocol: Assessment Report, United Nations Environment Programme, Nairobi, Kenya, 2021.

Vollmer, M., Zhou, L., Greally, B., Henne, S., Yao, B., Reimann, S., Stordal, F., Cunnold, D., Zhang, X., and Maione, M.: Emissions of ozone-depleting halocarbons from China, Geophysical Research Letters, 36, 2009.

Wan, D., Xu, J., Zhang, J., Tong, X., and Hu, J.: Historical and projected emissions of major halocarbons in China, Atmospheric Environment, 43, 5822-5829, 2009.

Wang, C., Shao, M., Huang, D., Lu, S., Zeng, L., Hu, M., and Zhang, Q.: Estimating halocarbon emissions using measured ratio relative to tracers in China, Atmospheric Environment, 89, 816-826, 2014.

Warszawski, L., Frieler, K., Huber, V., Piontek, F., Serdeczny, O., Zhang, X., Tang, Q., Pan, M., Tang, Y., and Tang, Q.: Center for International Earth Science Information Network—CIESIN—Columbia University. (2016). Gridded population of the World, Version 4 (GPWv4): Population density. Palisades. NY: NASA Socioeconomic Data and Applications Center (SEDAC). doi: 10. 7927/H4NP22DQ, Atlas of Environmental Risks Facing China Under Climate Change, 228, 2017.

Yao, B., Vollmer, M., Zhou, L., Henne, S., Reimann, S., Li, P., Wenger, A., and Hill, M.: In-situ measurements of atmospheric hydrofluorocarbons (HFCs) and perfluorocarbons (PFCs) at the Shangdianzi regional background station, China, Atmospheric Chemistry and Physics, 12, 10181-10193, 2012.

Yokouchi, Y., Taguchi, S., Saito, T., Tohjima, Y., Tanimoto, H., and Mukai, H.: High frequency measurements of HFCs at a remote site in east Asia and their implications for Chinese emissions, Geophysical research letters, 33, 2006.